

Supporting Information

Bi³⁺ acting both as electron and as hole trap in La-, Y-, and LuPO₄

Tianshuai Lyu* and Pieter Dorenbos

Delft University of Technology, Faculty of Applied Sciences, Department of Radiation Science and Technology, section Luminescence Materials, Mekelweg 15, 2629JB Delft, The Netherlands

*E-mail: T.lyu-1@tudelft.nl

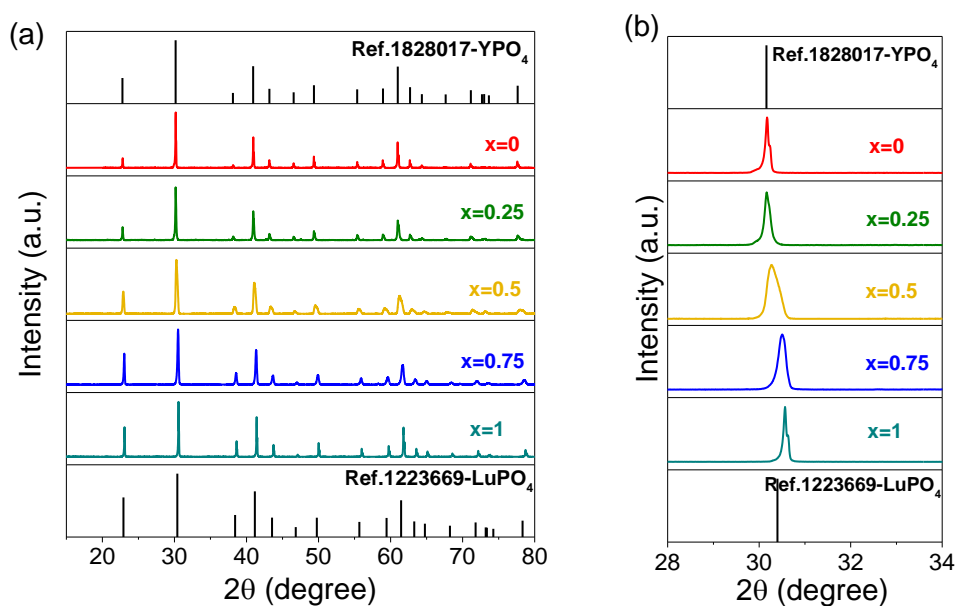


Fig. S1. (a) XRD patterns of $Y_{1-x}Lu_xPO_4:0.005Eu^{3+},0.005Bi^{3+}$ solid solutions ($x=0-1$). (b) detailed XRD patterns in the range from 28 to 34°.

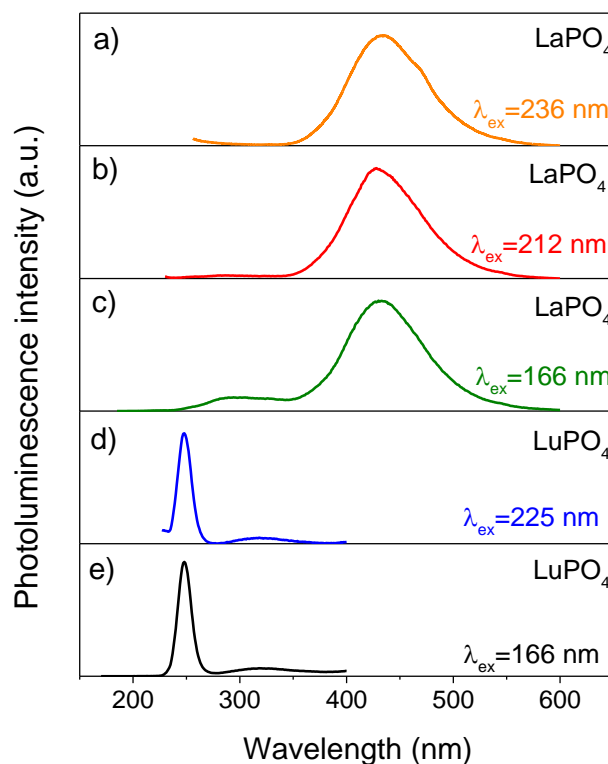


Fig. S2. Photoluminescence spectra of $LaPO_4:0.002Bi^{3+}$ and $LuPO_4:0.005Bi^{3+}$ excited at different excitation wavelength recorded at 10 K.

Fig. S2a-2c shows the photoluminescence spectra of $LaPO_4:0.002Bi^{3+}$ at different excitation wavelength. All spectra share a same band at 432 nm, and the weaker band at 288

nm only appears when excited at 166 nm and 212 nm. From the study by Boutinaud et al. [1], the band at 432 nm is tentatively attributed to $\text{CB} \rightarrow \text{Bi}^{3+}$ charge transfer emission.

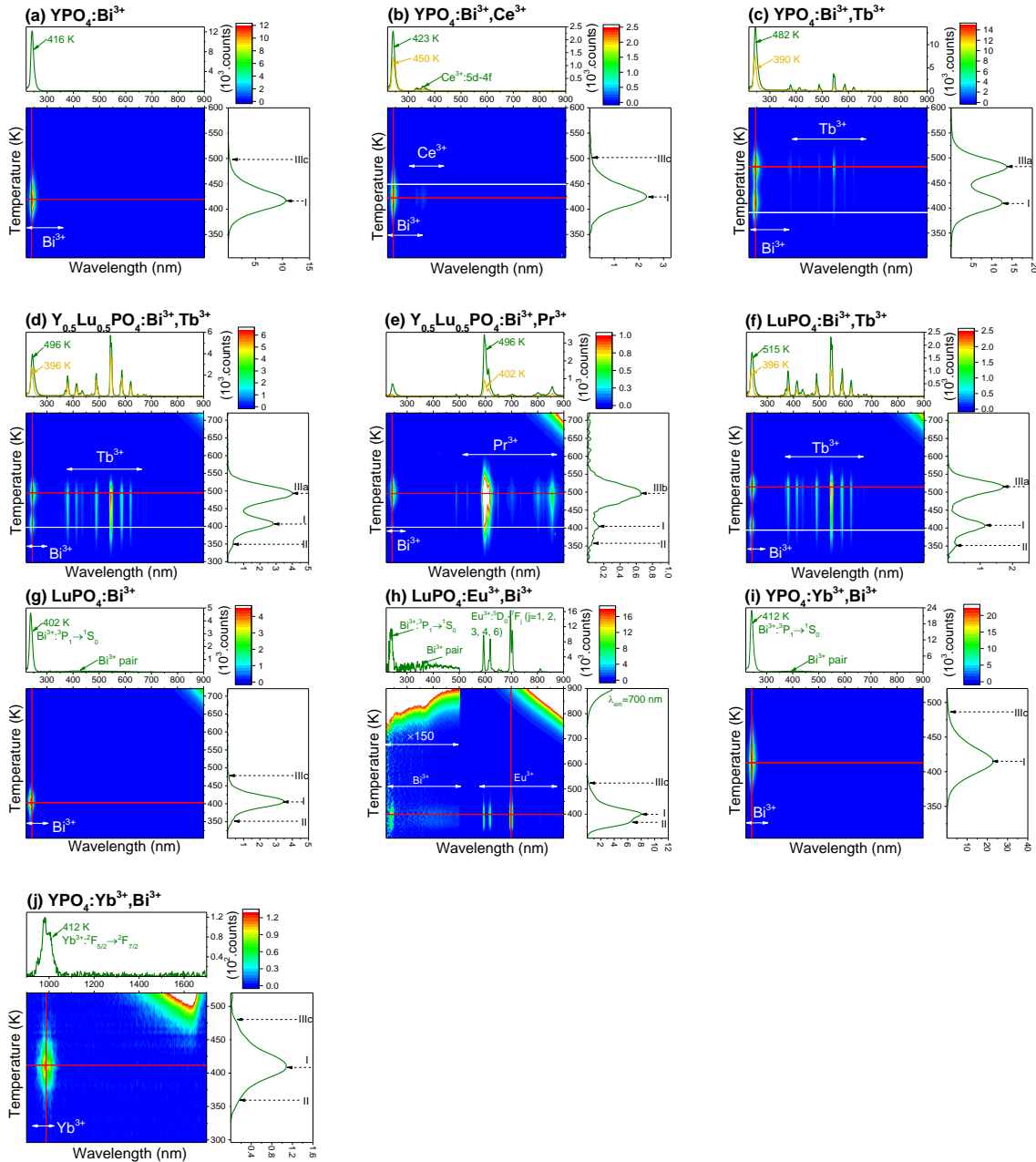


Fig. S3. Thermoluminescence emission (TLEM) plots of Bi^{3+} single or $\text{Bi}^{3+}\text{-Ln}^{3+}$ -codoped REPO_4 ($\text{RE}=\text{Y}$, and Lu ; $\text{Ln}=\text{Tb}$, Pr , Ce , Eu , and Yb) recorded at a heating rate of 1 K/s. The concentration of each dopant is fixed at 0.5 mol%.

The VRBE diagram in Fig. 1 predicts that Ce^{3+} acts as a 3.80 eV deep hole trapping center in $\text{YPO}_4:0.005\text{Bi}^{3+},0.005\text{Ce}^{3+}$ which is deeper than the 2.7 eV Bi^{3+} electron trapping center. The electron will be released earlier from Bi^{2+} than the hole from Ce^{4+} . One then can estimate according to Eq. (1) at the heating rate of 1 K/s that electron release from Bi^{2+} to the conduction band bottom in YPO_4 will give rise to a glow peak T_m at ~ 930 K.

With the VRBE at Bi^{2+} ground state between that of Sm^{2+} and Yb^{2+} we expect that the TL glow appears at between 679 and 965 K as observed for $\text{YPO}_4:\text{Ce}^{3+},\text{Ln}^{3+}$ ($\text{Ln}=\text{Sm}$, and Yb) in Ref [2]. Clearly, the Bi^{3+} electron trap is too deep to release an electron in the measurement range, which explains why no additional TL band(s) with Ce^{3+} emission appears in Fig. S3b.

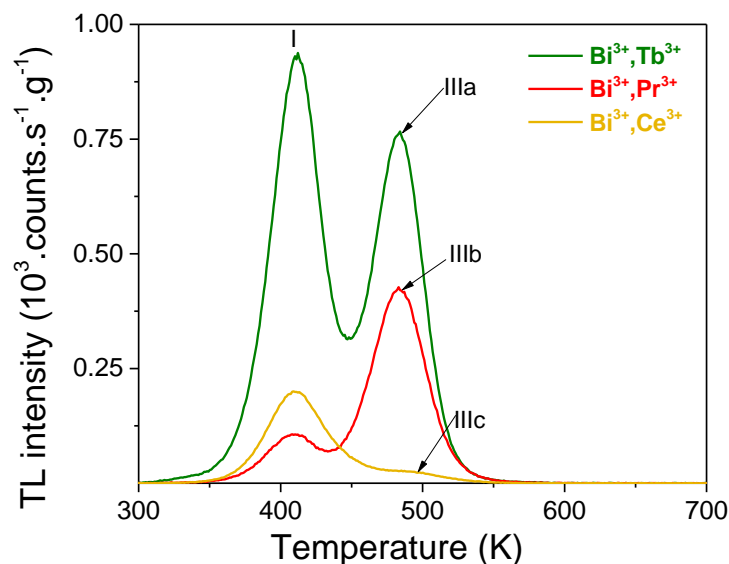


Fig. S4. TL glow curves of $\text{YPO}_4:0.005\text{Bi}^{3+},0.005\text{Ln}^{3+}$ ($\text{Ln}=\text{Tb}$, Pr , and Ce) samples recorded after 4000 s β irradiation monitoring Bi^{3+} emission at a heating rate of 1 K/s.

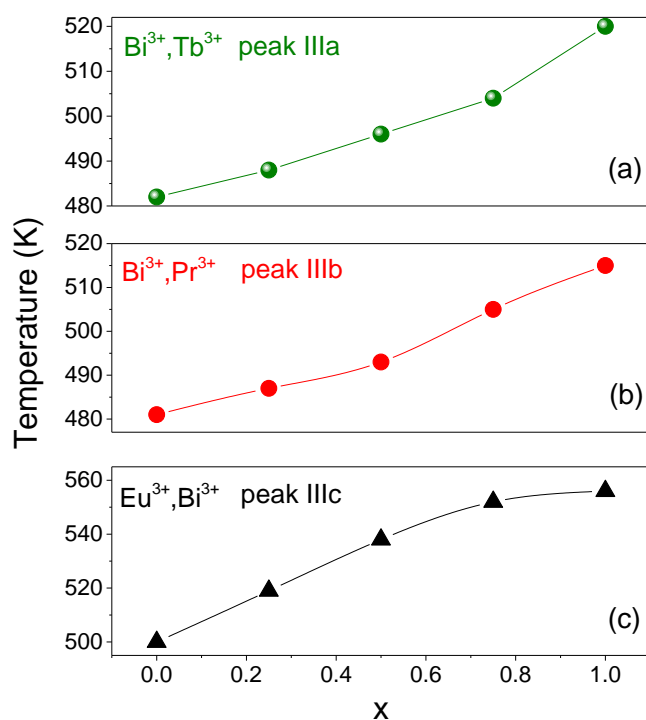


Fig. S5. Comparison of TL glow peaks IIIa, IIIb, and IIIc for $\text{Y}_{1-x}\text{Lu}_x\text{PO}_4:0.005\text{Bi}^{3+},0.005\text{Ln}^{3+}$ ($\text{Ln}=\text{Tb}$, and Pr) and $\text{Y}_{1-x}\text{Lu}_x\text{PO}_4:0.005\text{Eu}^{3+},0.005\text{Bi}^{3+}$ solid solutions ($x=0-1$).

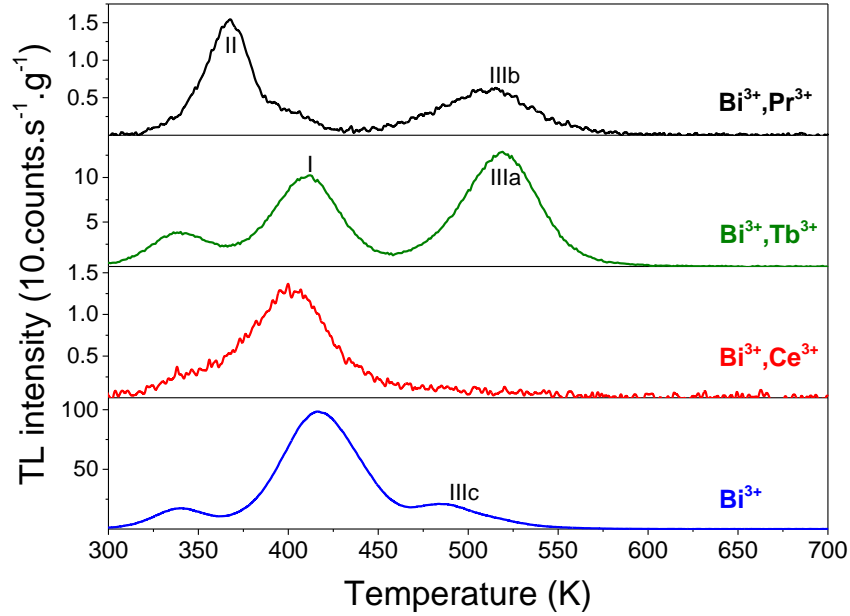


Fig. S6. TL glow curves of $\text{LuPO}_4:0.005\text{Bi}^{3+},0.005\text{Ln}^{3+}$ ($\text{Ln}=\text{Pr}$, Tb , and Ce) recorded after exposure to β source for 4000 s monitoring Bi^{3+} emission at a heating rate of 1 K/s.

Fig. S6 shows the TL glow curves for $\text{LuPO}_4:0.005\text{Bi}^{3+},0.005\text{Ln}^{3+}$ ($\text{Ln}=\text{Pr}$, Tb , and Ce) samples. Similar as in Fig. 3a and S4 for YPO_4 , Tb and Pr also give rise to two peaks IIIa and IIIb in $\text{LuPO}_4:0.005\text{Bi}^{3+},0.005\text{Tb}^{3+}$ and $\text{LuPO}_4:0.005\text{Bi}^{3+},0.005\text{Pr}^{3+}$. The TL glow curves of the single Bi^{3+} and the $\text{Bi}^{3+}\text{-Ce}^{3+}$ -codoped samples are shown to illustrate the absence of peaks IIIa and IIIb. These results further support that the glow peaks IIIa and IIIb are due to hole release from Tb^{4+} and Pr^{4+} and recombination on Bi^{2+} .

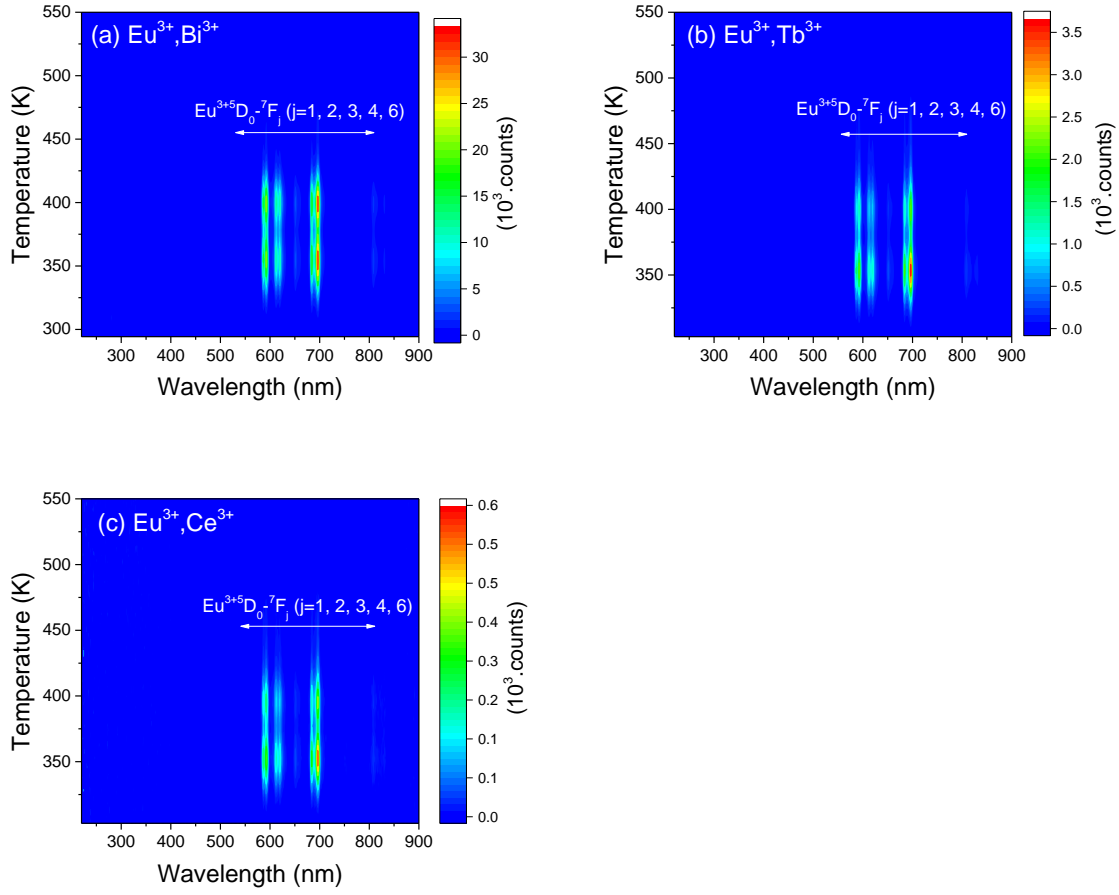


Fig. S7. Thermoluminescence emission (TLEM) plots of (a) $\text{LaPO}_4:0.005\text{Eu}^{3+},0.005\text{Bi}^{3+}$, (b) $\text{LaPO}_4:0.005\text{Eu}^{3+},0.005\text{Tb}^{3+}$, and (c) $\text{LaPO}_4:0.005\text{Eu}^{3+},0.005\text{Ce}^{3+}$ at a heating rate of 1 K/s.

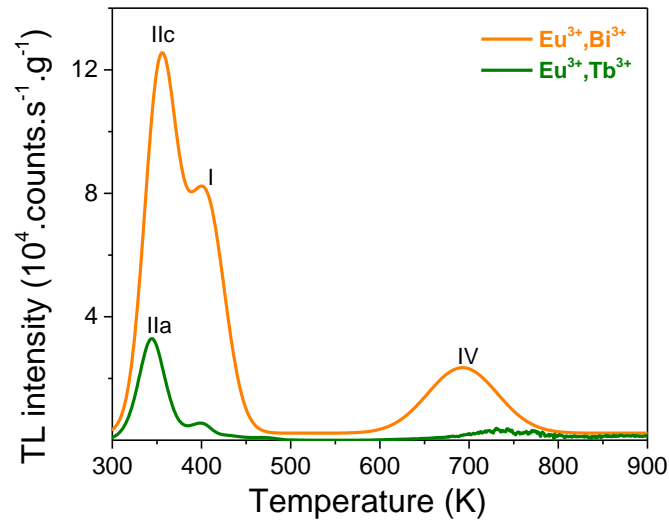


Fig. S8. (a) TL glow curves of $\text{LaPO}_4:0.005\text{Eu}^{3+},0.005\text{Bi}^{3+}$ and $\text{LaPO}_4:0.005\text{Eu}^{3+},0.005\text{Tb}^{3+}$ monitoring the red emission from Eu^{3+} recorded at a heating rate of 1 K/s. The data on $\text{LaPO}_4:0.005\text{Eu}^{3+},0.005\text{Tb}^{3+}$ were obtained from Lyu et al. [3].

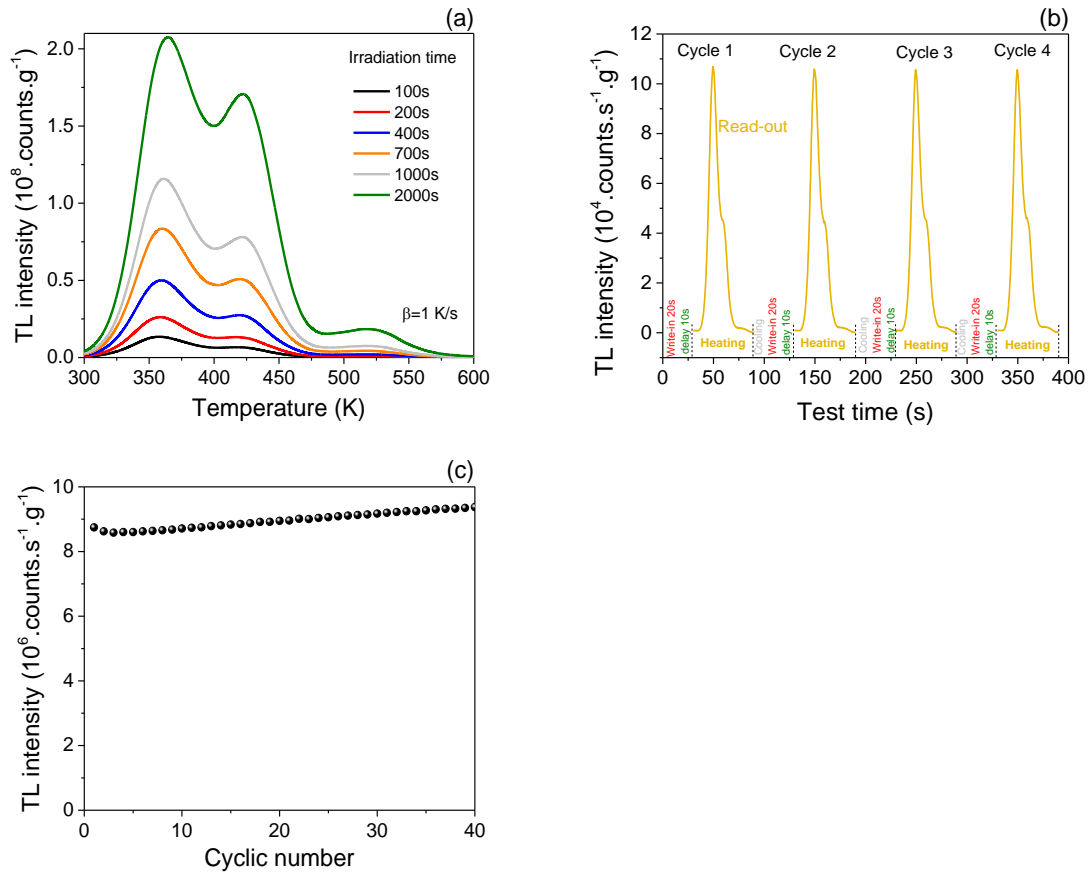


Fig. S9. (a) TL glow curves charged by β irradiation at different dose, (b) repeatability test of TL glow curves after 20 s β irradiation, and (c) integrated TL glow intensity as a function of cyclic number for $\text{LaPO}_4:0.005\text{Eu}^{3+},0.005\text{Bi}^{3+}$.

Fig. S9a shows the TL glow curves for $\text{LaPO}_4:0.005\text{Eu}^{3+},0.005\text{Bi}^{3+}$ charged by a β dose of 70 to 1400 mGy. All TL glow curves show their maxima at the same temperature $T_m (\pm 6 \text{ K})$, suggesting that the first-order TL recombination approximation is justified⁴.

Note that a proportional increase of the TL intensity appears when irradiation time increases. This shows that this phosphor has potential application as energy storing materials or as a dosimeter for detection of ionizing radiation. Fig. S9b shows a repeatability test of TL glow curves of $\text{LaPO}_4:0.005\text{Eu}^{3+},0.005\text{Bi}^{3+}$. The integrated TL intensities in Fig. S9c suggest that this phosphor is relatively stable during the 40 cycle test.

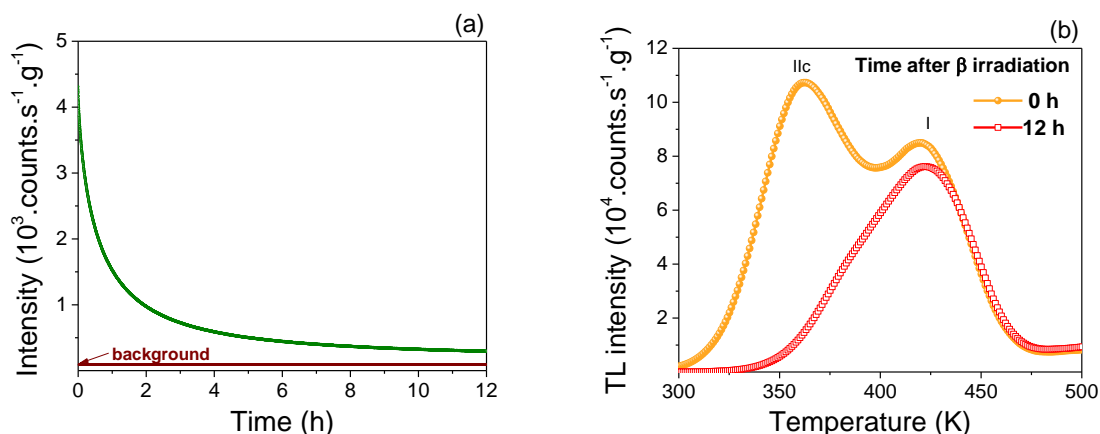


Fig. S10. (a). Isothermal decay curve monitoring the Eu^{3+} emission recorded at room temperature and (b) TL glow curves with different waiting time after 2000 s β irradiation for $\text{LaPO}_4:0.005\text{Eu}^{3+},0.005\text{Bi}^{3+}$.

Fig. S10a shows that the persistent luminescence from Eu^{3+} can still be detected after 12 h at RT. In order to identify the origin of the afterglow, Fig. S10b shows the TL glow curve of $\text{LaPO}_4:0.005\text{Eu}^{3+},0.005\text{Bi}^{3+}$ without and with 12 h waiting time after β irradiation. It shows that glow peak IIC disappears almost entirely after 12 h. This suggests that the hole release from a shallow host related hole trap at RT and recombination on Eu^{2+} may be responsible for the Eu^{3+} afterglow.

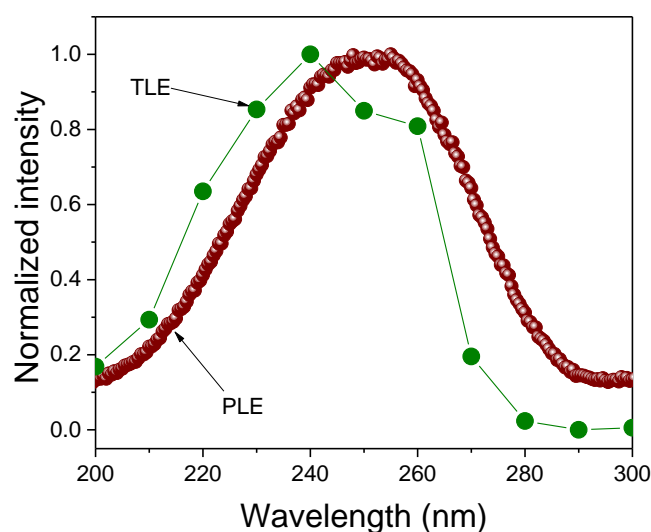


Fig. S11. Thermoluminescence excitation (TLE) spectrum of $\text{LaPO}_4:0.005\text{Eu}^{3+},0.005\text{Bi}^{3+}$ and photoluminescence excitation (PLE) spectrum of $\text{LaPO}_4:0.005\text{Eu}^{3+}$ monitoring the Eu^{3+} 590 nm emission recorded at room temperature.

TL excitation (TLE) spectra for $\text{LaPO}_4:0.005\text{Eu}^{3+},0.005\text{Bi}^{3+}$ were recorded by first illuminating the samples during 4000 s with a monochromatic photon beam generated using a 150 W xenon arc lamp (Hamamatsu L2273) filtered by a monochromator (Oriol Cornerstone

130). This system has a wavelength resolution of 0.8 nm against 0.1 mm slit width. The slit width was set to 1 mm and the wavelength step as 10 nm. A LabVIEW program was used to record TL glow curves in 300-700 K at a heating rate of 5 K/s when the excitation wavelengths change between 200 and 300 nm.

To investigate the origin of glow peaks I and IIc, Fig. S11 shows the thermoluminescence excitation (TLE) spectrum of the TL glow peak between 300-500 K for $\text{LaPO}_4:0.005\text{Eu}^{3+}, 0.005\text{Bi}^{3+}$. A broad TL excitation band extending from 200 to 300 nm and peaking at 240 nm is detected. The position and width resembles with the $\text{VB} \rightarrow \text{Eu}^{3+}$ charge transfer band of $\text{LaPO}_4:0.005\text{Eu}^{3+}$, where the band width is identical but it appears 10 nm blue shifted corresponding with 0.2 eV. During CT band excitation, electrons are excited from the valence band to $4f^7$ ($^8\text{S}_{7/2}$) of Eu^{2+} and holes are generated in the valence band which can then be trapped by host intrinsic hole trapping center. During TL readout, the holes release from hole trapping centers and then recombine with Eu^{2+} to yield Eu^{3+} 4f-4f emission. The 0.2 eV blue shift in band location may imply that the hole trap is far from Eu^{3+} , which is not conducive to hole release.

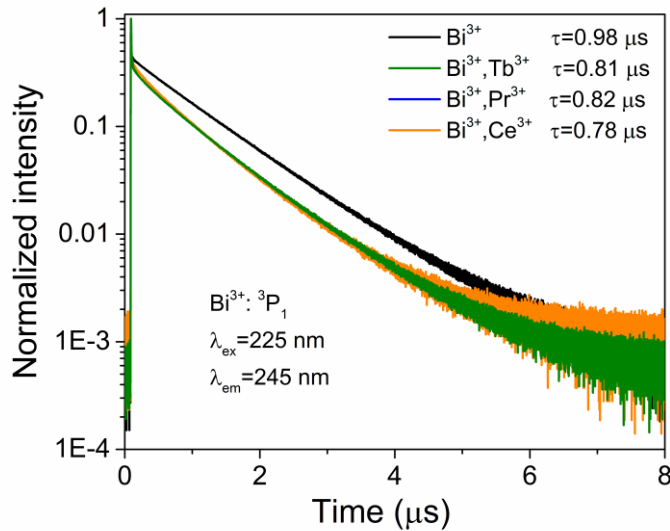


Fig. S12. Fluorescence lifetimes of $\text{YPO}_4:0.005\text{Bi}^{3+}, 0.005\text{Ln}^{3+}$ ($\text{Ln}=\text{Pr}, \text{Tb}, \text{and Ce}$) samples monitoring Bi^{3+} emission at 245 nm.

From the study in Ref. [5, 6] there are spectral overlaps between the Bi^{3+} A-band emission and the excitation bands of Ce^{3+} , Pr^{3+} , and Tb^{3+} , which suggests that there is a probability for the energy transfer from Bi^{3+} to Ce^{3+} , Pr^{3+} , or Tb^{3+} . To further show the energy transfer processes, Fig. S12 shows photoluminescence decay curves of the Bi^{3+} A-band emission in $\text{YPO}_4:0.005\text{Bi}^{3+}, 0.005\text{Ln}^{3+}$. For $\text{YPO}_4:0.005\text{Bi}^{3+}$, the decay curve can be well fitted by a single exponential function which can be written as

$$I(t) = I_0 \times \exp\left(-\frac{t}{\tau}\right) \quad (1)$$

where I_0 and I_t are emission intensities of a sensitizer Bi^{3+} in the absence and presence of an activator Ce^{3+} , Tb^{3+} , or Pr^{3+} , respectively. The lifetime of the Bi^{3+} A-band emission in $\text{YPO}_4:0.005\text{Bi}^{3+}$ is derived to be $0.98 \mu\text{s}$ using Eq. (1). With the co-doping of Ce^{3+} , Tb^{3+} , or Pr^{3+} , decay curves deviate from single exponential function and the Bi^{3+} lifetime decreases. This indicates that the co-doping Ln^{3+} modifies the luminescence dynamic of Bi^{3+} because of the energy transfer from Bi^{3+} to Ln^{3+} .

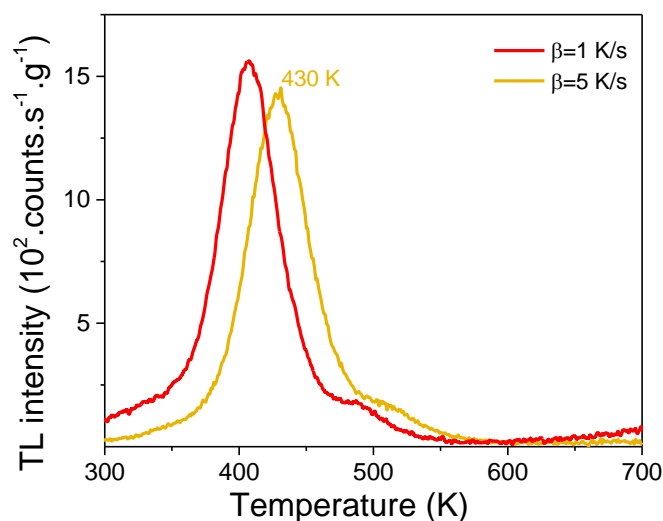


Fig. S13. TL glow curves of $\text{YPO}_4:0.005\text{Bi}^{3+},0.005\text{Ce}^{3+}$ recorded at different heating rates of 1 and 5 K/s after 400 s β source irradiation. A Hoya C5-58 filter was utilized to select Ce^{3+} emission.

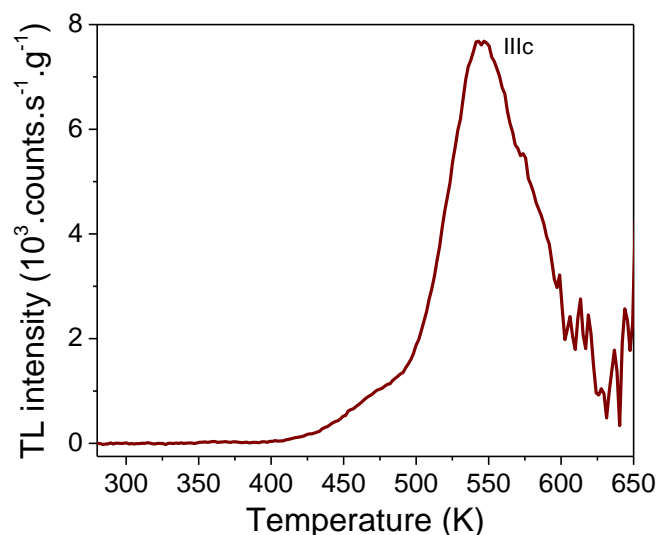


Fig. S14. TL glow curve of $\text{YPO}_4:0.005\text{Eu}^{3+},0.005\text{Bi}^{3+}$ charged by a laser beam at 212 nm for 600 s recorded at a heating rate of 5 K/s. The Eu^{3+} red emission was monitored.

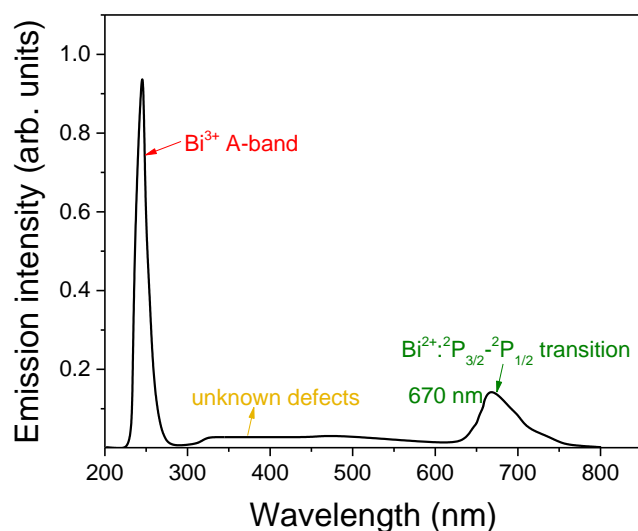


Fig. S15. X-ray excited emission spectrum for YPO₄: 0.05mol%Bi sample recorded at room temperature. The data were obtained from Awater et al. [10].

The emission band peaked at 670 nm has been ascribed in Ref. [10] to Bi²⁺ ²P_{3/2} → ²P_{1/2} transition, which is induced via the capturing of an electron from the conduction band by Bi³⁺ to form the excited state of Bi²⁺.

Reference

1. P. Boutinaud, *Inorganic Chemistry*, 2013, **52**, 6028-6038.
2. A. J. J. Bos, P. Dorenbos, A. Bessière, A. Lecointre, M. Bedu, M. Bettinelli and F. Piccinelli, *Radiation Measurements*, 2011, **46**, 1410-1416.
3. T. Lyu and P. Dorenbos, *Journal of Materials Chemistry C*, 2018, **6**, 369-379.
4. A. J. J. Bos, *Radiation Measurements*, 2006, **41**, S45-S56.
5. T. Jüstel, P. Huppertz, W. Mayr and D. U. Wiechert, *Journal of Luminescence*, 2004, **106**, 225-233.
6. W. Di, X. Wang, B. Chen, H. Lai and X. Zhao, *Optical Materials*, 2005, **27**, 1386-1390.
7. M. Jiao, Y. Jia, W. Lu, W. Lv, Q. Zhao, B. Shao and H. You, *Journal of Materials Chemistry C*, 2014, **2**, 90-97.
8. D. L. Dexter and J. H. Schulman, *The Journal of Chemical Physics*, 1954, **22**, 1063-1070.
9. G. Blasse, *Physics Letters A*, 1968, **28**, 444-445.
10. R. H. P. Awater, L. C. Niemeijer-Berghuijs and P. Dorenbos, *Optical Materials*, 2017, **66**, 351-355.